PHYSICAL REVIEW D **72,** 045014 (2005)

All next-to-maximally-helicity-violating one-loop gluon amplitudes in $\mathcal{N} = 4$ super-Yang-Mills theory

Zvi Bern
Department of Physics and Astronomy, UCLA, Los Angeles, California 90095-1547, USA

Lance J. Dixon
Stanford Linear Accelerator Center, Stanford University Stanford, California 94309, USA

David A. Kosower
Service de Physique Théorique, CEA-Saclay, F-91191 Gif-sur-Yvette cedex, France
(Received 9 February 2005; published 17 August 2005)

We compute the next-to-MHV one-loop n-gluon amplitudes in $\mathcal{N} = 4$ super-Yang–Mills theory. These amplitudes contain three negative-helicity gluons and an arbitrary number of positive-helicity gluons, and are the first infinite series of amplitudes beyond the simplest, MHV, amplitudes. We also discuss some aspects of their twistor-space structure.

DOI: 10.1103/PhysRevD.72.045014 PACS numbers: 11.15.Bt, 11.30.Pb, 11.55.Bq, 12.38.Bx

I. INTRODUCTION

The computation of on-shell amplitudes in the maximally-supersymmetric ($\mathcal{N} = 4$) gauge theory (MSYM) has proven to be a useful laboratory for developing computational techniques in perturbative gauge theories. Explicit results for amplitudes have in turn assisted the development of Witten's recent twistor-space topological string theory [1,2], a candidate for a weak–weak dual to the supersymmetric gauge theory. This string theory generalizes Nair's earlier description [3] of the simplest gauge-theory amplitudes. (Berkovits and Motl [4,5], Neitzke and Vafa [6], and Siegel [7] have given alternative descriptions of the candidate topological string theory.)

One-loop amplitudes in the maximally-supersymmetric theory can also be regarded as terms in a computation of amplitudes in perturbative QCD. In particular, the amplitudes where all external states are gluons can be decomposed into three terms, corresponding to the amplitude in the $\mathcal{N} = 4$ theory; to the contribution of a matter multiplet in the $\mathcal{N} = 1$ supersymmetric theory; and to the contribution of a scalar circulating in the loop. Moreover, in special cases, we show that coefficients of some integral functions in $\mathcal{N} = 4$ gauge theory are identical to those of QCD.

At tree level, three infinite sequences of gluon amplitudes were conjectured by Parke and Taylor [8] in the mid 1980s, and quickly proven by Berends and Giele [9]. Amplitudes with zero or one negative-helicity gluons, and an arbitrary number of positive helicity, vanish. Amplitudes with two negative-helicity gluons, so-called ''MHV'' amplitudes, have a very simple form.

Investigations of the twistor-space structure of known analytic results for more complicated helicity patterns led Cachazo, Svrček, and Witten (CSW) [10] to formulate a new set of rules for computing tree amplitudes in gauge theories. These rules employ vertices that are particular off-shell continuations of the MHV amplitudes. The vertices are sewn together using scalar propagators. These rules have made it straightforward to write down new analytic expressions for infinite sequences of amplitudes and currents with three or more negative-helicity legs, that is helicity configurations beyond MHV [10–14]. They have also been used to obtain amplitudes containing a Higgs boson coupled to QCD via a massive top-quark loop (in the infinite-mass limit) [15] and to obtain electroweak vector boson currents [16]. A natural question is whether one can compute similar amplitudes at one loop, and what light they shed on the structure of the twistor-space string dual to the gauge theory.

The unitarity-based method [17–20] makes use of the simple forms of tree amplitudes to produce, in turn, simple forms for infinite sequences of one-loop amplitudes. In this approach, we sew together products of on-shell tree amplitudes, and directly reconstruct Feynman integrals with the same analyticity properties. It makes use of the (standard) cuts of amplitudes, corresponding to the absorptive parts of amplitudes, and also introduces the nonstandard notion of generalized cuts [20–23] which has been used effectively in a variety of one- and two-loop calculations. We have employed both standard and generalized cuts for the calculations described in this paper. The unitarity-based techniques are enhanced by combining them with knowledge of the basis of dimensionally regularized one-loop integral functions that can appear in the results [17,24,25]. The basis required for one-loop $\mathcal{N} = 4$ super-Yang–Mills amplitudes is reproduced in appendix B. Knowledge of the basis reduces the problem to one of determining the coefficients in front of the integral functions. We have also made use of the requirement that the infrared divergences match the known universal form [26] for parts of the computation.

Recently, stimulated in part by the computation by Brandhuber, Spence and Travaglini [27] of the $\mathcal{N}=4$ MHV amplitudes from CSW diagrams [10], there has been a great deal of progress in obtaining and analyzing one-loop amplitudes in $\mathcal{N}=4$ and $\mathcal{N}=1$ theories using the unitarity method and twistor-motivated ideas [23,28–37]. These new results have also made it clear that the simplicity of tree amplitudes is inherited by their one-loop counterparts.

In this paper, we shall compute all next-to-MHV one-loop n-gluon amplitudes, that is one-loop amplitudes with three negative-helicity gluons and $(n-3)$ of positive-helicity. Some of the all-n coefficients appearing in the amplitudes were also computed elsewhere [23,31,36] These amplitudes in $\mathcal{N}=4$ super-Yang–Mills theory were computed previously for $n=6$ in Ref. [18], and for $n=7$ in Refs. [23,32]. For these two cases, using parity one can reduce the number of negative helicities to three or less; hence the next-to-MHV amplitudes exhaust the set of non-MHV amplitudes.

As a by-product of our computation, we have uncovered new representations of the NMHV n-point tree amplitudes. These representations arise from the required form of infrared divergences in any one-loop amplitude [26]. These new representations suggest that there is a more general formalism than MHV vertices for systematically and directly generating the tree amplitudes. The equivalence between the different representations appears to require a stronger symmetry than the gauge invariance needed to remove the CSW reference momentum.

This paper is organized as follows. In Sec. II, we describe our notation. Our calculational approach is discussed in Sec. III, with the results given in Sec. IV. Consistency checks on the results, as well as the derivation of a few sets of coefficients from collinear limits of ones obtained by direct calculation, are described in Sec. V. The new representations of n-point tree amplitudes, obtained from the infrared-divergent terms, are presented in Sec. VI. Finally, we discuss twistor-space properties of the box coefficients, for NMHV and more general amplitudes, in Sec. VII. Our conclusions and outlook are presented in Sec. VIII. We also include two appendices. The first contains an explicit demonstration that our all-n box coefficients are coplanar, as required [23,33]. The second contains the basis of box integral functions.

II. NOTATION

We use the trace-based color decomposition [38,39] of amplitudes. At tree level, this decomposition is,

$$\mathcal{A}_n^{\text{tree}}(\{k_i, h_i, a_i\}) = \sum_{\sigma\in S_n/Z_n} \text{Tr}(T^{a_{\sigma(1)}}\cdots T^{a_{\sigma(n)}}) A_n^{\text{tree}}(\sigma(1^{h_1},\ldots,n^{h_n})), \quad (1)$$

where S_n/Z_n is the group of noncyclic permutations on n symbols, and j^{h_j} denotes the j-th momentum and helicity h_j. The T^a are fundamental representation $\text{SU}(N_c)$ color matrices normalized so that $\text{Tr}(T^aT^b)=\delta^{ab}$. The color-ordered amplitude A_n^{tree} is invariant under a cyclic permutation of its arguments.

We describe the amplitudes using the spinor helicity formalism. In this formalism amplitudes are expressed in terms of spinor inner-products,

$$\begin{aligned}\langle jl\rangle &= \langle j^-|l^+\rangle = \bar{u}_-(k_j)u_+(k_l),\\ [jl] &= \langle j^+|l^-\rangle = \bar{u}_+(k_j)u_-(k_l),\end{aligned} \quad (2)$$

where $u_\pm(k)$ is a massless Weyl spinor with momentum k and plus or minus chirality [39,40]. Our convention is that all legs are outgoing. The notation used here follows the standard QCD literature, with $[ij]=\text{sign}(k_i^0k_j^0)\langle ji\rangle^*$ so that,

$$\langle ij\rangle[ji] = 2k_i\cdot k_j = s_{ij}. \quad (3)$$

(Note that the square bracket $[ij]$ differs by an overall sign compared to the notation commonly used in twistor-space studies [1].)

We denote the sums of cyclicly-consecutive external momenta by

$$K_{i\ldots j}^\mu \equiv k_i^\mu + k_{i+1}^\mu + \cdots + k_{j-1}^\mu + k_j^\mu, \quad (4)$$

where all indices are mod n for an n-gluon amplitude. The invariant mass of this vector is $s_{i\ldots j}=K_{i\ldots j}^2$. Special cases include the two- and three-particle invariant masses, which are denoted by

$$s_{ij}\equiv(k_i+k_j)^2 = 2k_i\cdot k_j, \qquad s_{ijk}\equiv(k_i+k_j+k_k)^2. \quad (5)$$

In color-ordered amplitudes only invariants with cyclicly-consecutive arguments need appear, e.g. $s_{i,i+1}$ and $s_{i,i+1,i+2}$. We also write, for the sum of massless momenta belonging to a set A,

$$K_A^\mu \equiv \sum_{a_i\in A} k_{a_i}^\mu. \quad (6)$$

(The sets that will appear in explicit expressions will be of cyclicly-consecutive external momenta.) For non-MHV loop amplitudes, longer spinor strings than (2) will typically appear, such as

$$\langle i^+|\not{K}_A|j^+\rangle \qquad \text{and} \qquad \langle i^-|\not{K}_A\not{K}_B|j^+\rangle. \quad (7)$$

The simplest color-ordered amplitudes are the maximally helicity-violating (MHV) Parke-Taylor tree amplitudes [8], which have two negative-helicity gluons and the rest of positive helicity,

$$A_{m_1m_2}^{\text{tree MHV}}(1,2,\ldots,n) = i\frac{\langle m_1m_2\rangle^4}{\langle 12\rangle\langle 23\rangle\cdots\langle n1\rangle}, \quad (8)$$

where $m_{1,2}$ label the negative-helicity legs.

For one-loop amplitudes, the color decomposition is similar to the tree-level case (1) [41]. When all internal particles transform in the adjoint representation of $SU(N_c)$, as is the case for $\mathcal{N} = 4$ supersymmetric Yang–Mills theory, we have

$$\mathcal{A}_n^{1-\text{loop}}(\{k_i, h_i, a_i\}) = \sum_{c=1}^{\lfloor n/2 \rfloor + 1} \sum_{\sigma \in S_n/S_{n;c}} \text{Gr}_{n;c}(\sigma) A_{n;c}(\sigma), \tag{9}$$

where $\lfloor x \rfloor$ is the largest integer less than or equal to x. The leading color-structure factor

$$\text{Gr}_{n;1}(1) = N_c \text{Tr}(T^{a_1} \cdots T^{a_n}), \tag{10}$$

is N_c times the tree color factor. The subleading color structures are given by

$$\text{Gr}_{n;c}(1) = \text{Tr}(T^{a_1} \cdots T^{a_{c-1}}) \, \text{Tr}(T^{a_c} \cdots T^{a_n}). \tag{11}$$

S_n is the set of all permutations of n objects, and $S_{n;c}$ is the subset leaving $\text{Gr}_{n;c}$ invariant.

The one-loop subleading-color partial amplitudes are given by a sum over permutations of the leading-color ones [17]. Therefore we need to compute directly only the leading-color single-trace partial amplitudes $A_{n;1}$.

The $\mathcal{N} = 4$ SYM amplitudes may be expressed as a sum of scalar box integrals I_4, multiplied by coefficients which are rational functions of spinor products [17]. It is convenient to multiply these integrals by suitable dimensionful combinations of kinematic invariants in order to obtain "box functions" F whose series expansions in ϵ only contain logarithmic or polylogarithmic dependence on the kinematic invariants. The necessary box functions $F^{4\text{m}}$, $F^{3\text{m}}$, $F^{2\text{m}h}$, $F^{2\text{m}e}$ and $F^{1\text{m}}$ (and for $n = 4$, $F^{0\text{m}}$), are listed in appendix B. The kinematics of each box function appearing in an n-point amplitude is determined by canceling $(n - 4)$ propagators from the n-point diagram with external legs in the order $1, 2, 3, \ldots, n$. In Ref. [23] we labeled the box integrals for $n = 7$ by a triplet of integers, say (i', j', k'), corresponding to the three propagators canceled from the heptagon diagram with external legs in the order $1, 2, 3, \ldots, 7$. This labeling scheme becomes very cumbersome for discussing the all-n case, since the number of integers required grows with n. Here we therefore choose to label the integrals, and their kinematic coefficients, by a *quartet* (i, j, k, l) of distinct integers, corresponding to the four *uncanceled* propagators. In the seven-point case, this quartet is the complement of the triplet (i', j', k') used in Ref. [23], $\{i, j, k, l\} \cup \{i', j', k'\} = \{1, 2, 3, 4, 5, 6, 7\}$. See Fig. 1 for examples of this labeling. (We also use the notation $B(i, j, k, l)$ for the labeled box functions, instead of $F(i, j, k, l)$, in order to avoid confusion with the twistor-space colinear operator F_{ijk} discussed in Sec. VII A.)

We write the $\mathcal{N} = 4$ leading-color partial amplitude as [17,24,25]

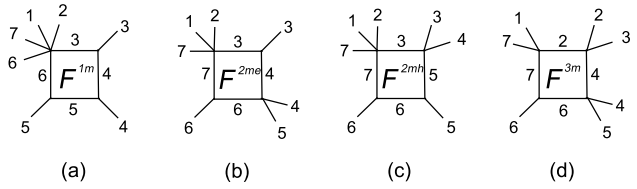

FIG. 1. Examples of box integral functions $B(i, j, k, l)$ appearing in seven-point amplitudes; the arguments i, j, k, l are the uncanceled propagators: (a) the one-mass box $B(3, 4, 5, 6) = F^{1\text{m}}(s_{34}, s_{45}, s_{345})$, (b) the "easy" two-mass box $B(3, 4, 6, 7) = F^{2\text{m}e}(s_{345}, s_{456}, s_{45}, s_{712})$, (c) the "hard" two-mass box $B(3, 5, 6, 7) = F^{2\text{m}h}(s_{56}, s_{345}, s_{712}, s_{34})$, and (d) the three-mass box $B(2, 4, 6, 7) = F^{3\text{m}}(s_{671}, s_{456}, s_{71}, s_{23}, s_{45})$.

$$A_{n;1}^{\mathcal{N}=4} = i\hat{c}_\Gamma(\mu^2)^\epsilon \sum_{i,j,k,l} c_{ijkl} B(i, j, k, l), \tag{12}$$

where c_{ijkl} is the kinematic coefficient and

$$\hat{c}_\Gamma = \frac{1}{(4\pi)^{2-\epsilon}} \frac{\Gamma(1 + \epsilon)\Gamma^2(1 - \epsilon)}{\Gamma(1 - 2\epsilon)} \tag{13}$$

is a ubiquitous prefactor, and $(\mu^2)^\epsilon$ is the trivial scale dependence of all dimensionally-regulated one-loop amplitudes. While the $\mathcal{N} = 4$ theory is ultraviolet-finite, on-shell amplitudes still have infrared divergences which are also regulated dimensionally, and sneak in a dependence on μ.

For a given helicity amplitude, the number of box functions, and box coefficients, is the number of unordered quartets of distinct integers (i, j, k, l) with each integer running from 1 to n, and all four unequal. This number is just $\binom{n}{4}$. These include,

(i) one-mass boxes shown in Fig. 1(a) (n boxes),
(ii) the easy two-mass boxes shown in Fig. 1(b), plus cyclic permutations ($n(n - 5)/2$ boxes in total),
(iii) the hard two-mass boxes shown in Fig. 1(c) ($n(n - 5)$ boxes),
(iv) the three-mass box shown in Fig. 1(d) ($n(n - 5) \times (n - 6)/2$ boxes).

We take the three negative-helicity gluons to be labeled by m_1, m_2, m_3.

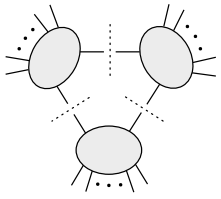

FIG. 2. A generalized triple cut. The three propagators cut by the dashed lines are required to be "open".

III. CALCULATIONAL APPROACH

Computing an infinite series of amplitudes would require computing an infinite number of Feynman diagrams. The unitarity-based method, however, can reduce such a computation to a finite one. We use it.

In the unitarity-based method, we reconstruct a loop amplitude from tree amplitudes by requiring that internal propagators go on shell. Letting two propagators go on shell corresponds to extracting the absorptive parts, which are just phase-space integrals over products of tree amplitudes. In most cases it is convenient to also use generalized cuts [20–23], where multiple propagators go on shell, such as the triple cut shown in Fig. 2. Taking a generalized cut corresponds to extracting those contributions to a loop amplitude where all cut propagators are required to be present. The generalized cuts have the property of reducing the building blocks of loop computations to the simplest possible set of tree amplitudes. They can even reduce higher-loop calculations to integrals over products of tree amplitudes [20,22]. In all cases, one reconstructs the loop integrals giving rise to the required ordinary or generalized cuts. In the present calculation, that only requires identifying the appropriate integral in the basis set.

Our coefficients were entirely obtained from the generalized triple and quadruple cuts by augmenting them with infrared consistency conditions as well as collinear and soft behaviors. The soft and collinear limits allow us to obtain unknown coefficients from explicitly computed ones. When required infinite series of tree-level amplitudes are known, the unitarity method enables us to compute infinite series of one-loop amplitudes. The combination of the various methods allows us to give explicit formulæ for all coefficients in NMHV n-point amplitudes.

In general, we must compute these cuts in D dimensions. For one-loop amplitudes in supersymmetric theories, however, it suffices to compute them in four dimensions [17,18]. (The reconstructed loop integral is still computed in D dimensions, of course.) The four-dimensional amplitudes are most efficiently and conveniently handled in a helicity basis. Starting from tree *amplitudes* rather than *diagrams* means that the extensive cancellations that occur in gauge theories are taken into account before any loop integrations are done, which greatly reduces the complexity of the calculations.

In extracting the triple cut, terms which vanish as the cut propagators go on shell may be dropped. The utility of this procedure comes from two aspects: the triple cut itself may be represented as a product of three tree amplitudes; and the resulting expression isolates coefficients of a more limited class of integrals than the ordinary (absorptive) cut. In the calculations we perform, these coefficients turn out to be the simplest of all integral coefficients (and even simple in an absolute sense). All three-mass and hard two-mass box coefficients may be determined from a triple cut. In an NMHV loop amplitude, each tree amplitude making up a triple cut will be an MHV amplitude, that is with two negative-helicity gluons, be they external or (cut) internal ones.

The quadruple cuts show very simply that all four-mass box coefficients must vanish in an NMHV amplitude. These cuts are given by products of four tree amplitudes. However, there are only seven negative-helicity gluon legs available: three are external gluons, and four are gluons crossing the cuts (one for each of the four cuts). Hence at least one of the four tree amplitudes must have fewer than two negative-helicity gluons, and will therefore vanish.

Having determined the three-mass and hard two-mass box coefficients from the triple cuts (or equivalently the ordinary cuts), we can determine the easy two-mass and one-mass coefficients in two independent ways. The first is to return to the ''ordinary'' cuts, and compute them. In this case, we will have the product of an MHV and an NMHV amplitude forming the cut. Depending on the configuration of the external negative-helicity gluons (and on the channel we cut), contributions will come either from gluons alone circulating in the loop (a ''singlet'' contribution) or from all states in the $\mathcal{N} = 4$ multiplet (''nonsinglet''). The tree-level CSW rules make it easy to write down analytic expressions for the NMHV amplitudes, but unfortunately the form they yield—containing off-shell momenta either in the original CSW form or in the modified ''projected'' form—is not directly suitable for use in the unitarity-based method, because it is not clear what propagators should be reconstructed from these unusual denominators. For the gluon amplitudes, however, a corresponding expression in terms of on-shell spinor products and invariants alone is known [12], and it is this expression we have used in computing the cuts. This provides a computation of the (subset of) easy two-mass and one-mass box coefficients that have singlet cuts, that is which have a cut that isolates all three negative helicities on one side of the cut. The calculation starts with an octagon integrand, which reduces to a sum of box integrands via spinor algebra and the introduction of appropriate ''cubic'' invariants [23]. Brute-force integral reduction techniques (e.g. Brown-Feynman or Passarino-Veltman [42]), which introduce nasty spurious Gram-determinant denominators, were not required.

The other method of determining these coefficients is to use the infrared consistency equations. These equations arise from confronting our knowledge of the structure of infrared singularities in the amplitude with the presence of singularities in individual box functions. On general grounds [26], we know that only nearest-neighbor two-particle invariants can appear in infrared-singular terms, which have the form,

$$A_{n;1}^{\mathcal{N}=4}|_{\epsilon\ \mathrm{pole}} = -\frac{\hat{c}_\Gamma}{\epsilon^2}\sum_{i=1}^{n}\left(\frac{\mu^2}{-s_{i,i+1}}\right)^{\epsilon} \times A_n^{\mathrm{tree}}, \qquad (14)$$

where μ is an arbitrary scale. On the other hand, the box

functions listed in appendix B contain singularities with coefficients $s^{-\epsilon}$ for a much larger set of invariants s. In general, Eq. (14) implies that the coefficient of any given $\ln(-s_{i,i+1})/\epsilon$ must be equal to the tree; and the coefficient of any other $\ln(-s_{i\ldots j})/\epsilon$ must vanish. Both types of equation are nontrivial. There are $n(n-3)/2$ such equations corresponding to the number of independent kinematic invariants. Each box function, listed in appendix B, contains various $\ln(-s_{i,i+1})/\epsilon$ and $\ln(-s_{i,i+1,i+2})/\epsilon$ terms with coefficients 0, ± 1 or $\pm\frac{1}{2}$. The constraints arising from Eq. (14) thus become simple linear relations among the coefficients, some of which involve the tree amplitude. As mentioned at the end of Sec. II there are a total of n one-mass boxes and $n(n-5)/2$ easy two-mass boxes, which together precisely match the number of infrared consistency equations.

It turns out that for n odd the system of equations is nondegenerate (verified numerically up to $n = 29$), so using the infrared consistency equations we can solve for *all* easy two-mass and one-mass box coefficients in terms of the three-mass and hard two-mass ones. For n even it turns out that there is one redundant equation, so that we can solve for all but one easy two-mass or one-mass box coefficient. Of course, once we have obtained the solution for odd n, we can confirm that the solution also holds for even n by taking collinear limits, as we shall mention in Sec. V. The solutions obtained from the infrared consistency equations, as it turns out, yield a simpler analytic (but numerically identical) form for the singlet coefficients than the direct computation discussed above. We have also used these infrared consistency equations to obtain the nonsinglet easy two-mass and one-mass coefficients.

IV. RESULTS

In this section we present the results for the box coefficients c_{ijkl} appearing in Eq. (12). It is convenient to label the coefficients in terms of clusters. For $X = A, B, C$, let X_1 denote the first massless momentum in X, and X_{-1} the last massless momentum.

As mentioned in the previous section, from the generalized quadruple cuts we see that the four-mass box coefficients all vanish.

The three-mass box coefficients are all given by a single ''term''. This simplicity is tied to the very constrained twistor-space structure of such coefficients. A three-mass box integral has a unique massless ''singlet'' leg s, followed clockwise around the loop by three massive clusters A, B and C, as shown in Fig. 3(d). (The momenta within each cluster are of course also ordered clockwise.) Then the three-mass box coefficient is given by,

$$\begin{aligned} c^{3\mathrm{m}}(m_1, m_2, m_3; s, A, B, C) &= \frac{[\mathcal{H}(m_1, m_2, m_3; s, A, B, C)]^4}{\langle 12\rangle\langle 23\rangle\cdots\langle n1\rangle K_B^2} \\ &\times \frac{\langle A_{-1}B_1\rangle}{\langle s^-|\not{K}_C\not{K}_B|A_{-1}^+\rangle\langle s^-|\not{K}_C\not{K}_B|B_1^+\rangle} \\ &\times \frac{\langle B_{-1}C_1\rangle}{\langle s^-|\not{K}_A\not{K}_B|B_{-1}^+\rangle\langle s^-|\not{K}_A\not{K}_B|C_1^+\rangle}, \end{aligned} \tag{15}$$

where all the dependence on the m_i is contained within $\mathcal{H}$. In the cases where the singlet leg s has positive helicity, we find,

$$\mathcal{H} = 0, \qquad m_{1,2,3} \in A, \tag{16}$$

$$= 0, \qquad m_{1,2,3} \in B, \tag{17}$$

$$= \langle m_1 m_2\rangle\langle s^-|\not{K}_C\not{K}_B|m_3^+\rangle, \qquad m_{1,2} \in A, m_3 \in B, \tag{18}$$

$$= \langle m_1 m_2\rangle\langle s m_3\rangle K_B^2, \qquad m_{1,2} \in A, m_3 \in C, \tag{19}$$

$$= \langle m_1 m_2\rangle\langle s^-|\not{K}_C\not{K}_B|m_3^+\rangle, \qquad m_{1,2} \in B, m_3 \in A, \tag{20}$$

$$= \langle m_1 m_2\rangle\langle s^-|\not{K}_A\not{K}_B|m_3^+\rangle + \langle m_3 m_2\rangle\langle s^-|\not{K}_C\not{K}_B|m_1^+\rangle, \quad m_1 \in A, m_2 \in B, m_3 \in C, \tag{21}$$

plus cases obtained by exchanging A and C (using reflection/flip symmetry). An alternative form for the last case is,

$$\mathcal{H} = \langle s m_1\rangle\langle m_3^-|(\not{K}_s + \not{K}_C)\not{K}_B|m_2^+\rangle + \langle s m_3\rangle \times \langle m_1^-|\not{K}_A\not{K}_B|m_2^+\rangle, \qquad m_1 \in A, m_2 \in B, m_3 \in C. \tag{22}$$

In the cases where the singlet leg has negative helicity, $s = m_3$, we find,

$$\mathcal{H} = 0, \qquad m_{1,2} \in A, \tag{23}$$

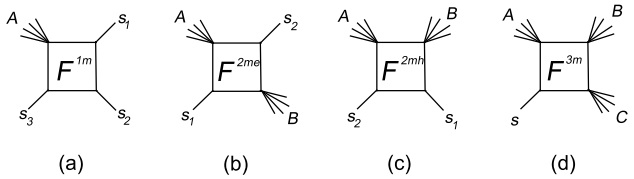

FIG. 3. The box integral functions labeled by the clusters of masses.

$$= \langle m_1 m_2 \rangle \langle s^- | \not{K}_C \not{K}_B | s^+ \rangle, \qquad m_{1,2} \in B, \tag{24}$$

$$= \langle s m_1 \rangle \langle s^- | \not{K}_C \not{K}_B | m_2^+ \rangle, \qquad m_1 \in A, m_2 \in B, \tag{25}$$

$$= \langle s m_1 \rangle \langle s m_2 \rangle K_B^2, \qquad m_1 \in A, m_2 \in C, \tag{26}$$

plus cases obtained by exchanging A and C.

All the other box coefficients are given by appropriate sums of c^{3m} quantities. In many instances, Eq. (15) will then be required when the set A or C "degenerates" to a single leg. ($X_1 = X_{-1} = X$ if the cluster degenerates to a single massless momentum.) The formula is perfectly well-defined in this limit. On the other hand, the set B will never be allowed to degenerate to a single leg, because the K_B^2 factor in the denominator of Eq. (15) would then vanish. In the following equations, $m_{1,2,3}$ do not play any distinguished role, and for simplicity we shall suppress these arguments.

The hard two-mass boxes are defined by two adjacent singlet legs, s_1 and s_2, followed by two adjacent massive clusters A and B, as shown in Fig. 3(c). Their coefficients are given simply by the sum of two c^{3m}s:

$$c^{2mh}(s_1, s_2, A, B) = c^{3m}(s_1, \{s_2\}, A, B) + c^{3m}(s_2, A, B, \{s_1\}). \tag{27}$$

In Sec. V we will confirm this formula using soft limits.

The easy two-mass boxes are defined by a singlet leg s_1 followed cyclicly by a massive cluster A, then another singlet leg s_2, then a final massive cluster B, as shown in Fig. 3(b). They are given by a pair of double sums over c^{3m} coefficients. In the first sum, leg s_1 is treated as a singlet, the first massive cluster must include s_2, and the second massive cluster must not degenerate to a massless leg. Otherwise there are no restrictions on the sum. The second sum can be obtained from the first sum by exchanging the roles of $s_1 \leftrightarrow s_2$ and $A \leftrightarrow B$. The result is,

$$c^{2me}(s_1, A, s_2, B) = \sum_{k=0}^{M(s_1,s_2)} \sum_{l=0}^{M(s_1,s_2)-k} c^{3m}(s_1, \hat{A}(s_1, s_2, k), \hat{B}(s_1, s_2, k, l), \hat{C}(s_1, s_2, k, l)) + \sum_{k=0}^{M(s_2,s_1)} \sum_{l=0}^{M(s_2,s_1)-k} c^{3m}(s_2, \hat{A}(s_2, s_1, k), \hat{B}(s_2, s_1, k, l), \hat{C}(s_2, s_1, k, l)), \tag{28}$$

where

$$\hat{A}(s_1, s_2, k) = \{s_1 + 1, \ldots, s_2 + k\}, \tag{29}$$

$$\hat{B}(s_1, s_2, k, l) = \{s_2 + k + 1, \ldots, s_2 + k + l + 2\}, \tag{30}$$

$$\hat{C}(s_1, s_2, k, l) = \{s_2 + k + l + 3, \ldots, s_1 - 1\}, \tag{31}$$

and

$$M(s_1, s_2) = n - 4 - [(s_2 - s_1) \bmod n]. \tag{32}$$

A schematic depiction of the double sum (28) is provided in Fig. 4. Note that there is a certain cyclic "handedness" to the sum, in that the "buried" leg s_2 is clockwise from the singlet leg s_1 in the first sum, and similarly in the second sum. There is an alternative representation where this handedness is reversed, which we have numerically verified to be equivalent.

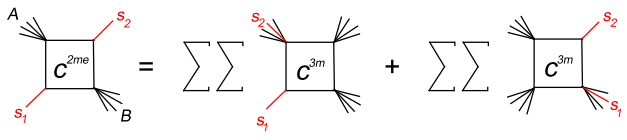

FIG. 4 (color online). Schematic depiction of the easy two-mass box coefficients, expressed as a double sum over three-mass box coefficients.

The one-mass boxes are defined by three adjacent singlet legs, s_1, s_2 and s_3, followed by a massive cluster A, as shown in Fig. 3(a). Their coefficients are given by the degeneration of the easy two-mass formula, plus a single additional term:

$$c^{1m}(s_1, s_2, s_3, A) = c^{2me}(s_1, \{s_2\}, s_3, A) + c^{3m}(s_2, \{s_3\}, A, \{s_1\}). \tag{33}$$

Many of the above coefficients also carry over to the corresponding amplitudes in QCD. We can apply the generalized cuts to determine which coefficients in QCD are identical to those given above. Many types of integral functions beyond those appearing in the $\mathcal{N} = 4$ results also contribute to the full QCD results—scalar triangle integrals, scalar and tensor bubble integrals—and their coefficients are of course undetermined by the calculations in this paper. Let us assume that we are working in a basis of integrals where the only box integrals appearing are those in $D = 4 - 2\epsilon$. Whenever a box coefficient can be determined from a (generalized) cut in which *only gluons* are allowed to propagate around the loop, then the fermion and scalar contributions are absent, and the QCD coefficient is exactly the same as the coefficient in $\mathcal{N} = 4$

super-Yang–Mills theory. Suppose, for example, a box integral has a massive leg out of which only positive-helicity gluons flow. Inspecting the cut which separates that leg from the rest of the amplitude, we see that only gluons can contribute. Thus having an "all-plus mass" is a sufficient condition for a box coefficient in QCD (or in the pure-glue theory) to be determined by the $\mathcal{N} = 4$ formula given in this section. It is worth noting that amongst the three-mass boxes, the only case which does *not* satisfy this condition is $m_1 \in A$, $m_2 \in B$, $m_3 \in C$ (Eq. (21)). In the cases of the hard two-mass and one-mass boxes, for QCD and $\mathcal{N} = 4$ super-Yang–Mills theory to give the same result, another sufficient condition is that two adjacent massless legs have the same helicity.

V. CONSISTENCY OF THE RESULTS

We have performed a number of nontrivial checks on the amplitudes. One simple check is against all previously computed [17,23,32] $\mathcal{N} = 4$ amplitudes, when the number of legs n is taken to be six or seven. Another check, discussed in Sec. III and valid beyond $n = 7$, is our computation of many of the easy two-mass and one-mass box coefficients in two independent ways, using the infrared consistency conditions and also direct computation.

Amplitudes are constrained by a variety of nontrivial requirements. Their analytic properties are tightly constrained because all kinematic poles and cuts must correspond to propagation of physical particles. They must also have infrared singularities corresponding to the universal emission of soft and collinear gluons.

In the collinear region, $k_a \to z k_P$, $k_b \to (1-z) k_P$, where k_P is the momentum of the quasi-on-shell intermediate state P, with helicity h. In this limit, massless color-ordered tree amplitudes behave as

$$A_n^{\text{tree}} \xrightarrow{a\|b} \sum_{h=\pm} \text{Split}^{\text{tree}}_{-h}(z, a^{h_a}, b^{h_b}) A^{\text{tree}}_{n-1}(\ldots (a+b)^h \ldots), \tag{34}$$

where $\text{Split}^{\text{tree}}_{-h}$ are tree-level splitting amplitudes [39]. At one loop, the generalization is,

$$A^{1-\text{loop}}_{n;1} \xrightarrow{a\|b} \sum_{h=\pm} (\text{Split}^{\text{tree}}_{-h}(z, a^{h_a}, b^{h_b}) A^{1-\text{loop}}_{n-1;1}(\ldots (a+b)^h \ldots) + \text{Split}^{1-\text{loop}}_{-h}(z, a^{h_a}, b^{h_b}) A^{\text{tree}}_{n-1}(\ldots (a+b)^h \ldots)), \tag{35}$$

where the $\text{Split}^{1-\text{loop}}_{-h}$ are one-loop splitting amplitudes, which are tabulated in the second appendix of Ref. [17]. This reference also contains a discussion of the behavior of the collinear limits of one-loop amplitudes and integral functions. We will refer to the original amplitude as the "parent" and the resulting amplitude appearing in the collinear limit as the "daughter" amplitude.

Besides providing nontrivial checks, collinear limits also allow us to fill a small gap in our calculation of coefficients using the infrared consistency conditions, which appears when the number of legs is even. Recall that as discussed in Sec. III, for even n there is one redundant equation, and accordingly we are missing one equation needed to completely determine the easy two-mass and one-mass box coefficients (which we collectively refer to as "easy-class"). For odd n we have exactly the right number of equations. One simple way around this problem is to prove the correctness of coefficients for even n by taking the collinear limits of the $(n+1)$-point (odd) case. Because we are missing only one equation, the confirmation of even a single easy-class coefficient is sufficient to prove that our solution is complete. We can therefore choose the simplest collinear limits to evaluate. A suitably simple limit arises when the two color-adjacent legs becoming collinear, a and b, both have positive helicity, and are buried inside a cluster in the parent easy two-mass box-coefficient, as shown in Fig. 5. If a or b is adjacent to one of the massless legs of the easy two-mass box, the analysis is more complicated, but we do not need to consider such cases.

According to Eq. (35), there are contributions proportional to the one-loop splitting function $\text{Split}^{1-\text{loop}}$ as well as those proportional to the tree splitting function $\text{Split}^{\text{tree}}$. Let us examine the latter terms, because their contributions are entirely dictated by the collinear behavior of the box coefficients $c^{2m\epsilon}$.

To understand the collinear limits we need to inspect the easy two-mass box coefficients. These coefficients are sums of three-mass box coefficients, as given in Eq. (28). In a given term in the sum, if a and b belong to a single mass of the coefficient c^{3m} with three or more legs in the mass, it maps very simply into the terms in the daughter sum because only sums of momenta in the parent cluster appear in the formula (15), i.e., $k_a + k_b \to k_P$ in the daughter coefficient. We obtain an overall tree splitting amplitude factor of $1/(\sqrt{z(1-z)}\langle ab\rangle)$, coming from the

$$\frac{1}{\langle 12\rangle\langle 23\rangle \cdots \langle n1\rangle} \tag{36}$$

prefactor of the coefficient.

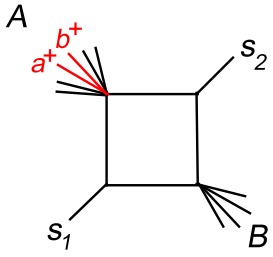

FIG. 5 (color online). An easy two-mass box where positive-helicity legs a and b are buried inside a cluster.

There are, however, some special cases to consider. Suppose that in the given term under consideration in the sum, a and b are the only legs in one of the massive cluster arguments to c^{3m}. If the (a, b) cluster is A or C, corresponding to Fig. 3, then the limit works as above, because massless legs are allowed in the sum over three-mass coefficients if they are in the A or C position. If a and b are the only members of B, then in the collinear limit there is no corresponding daughter coefficient in the sum, so all such coefficients must be nonsingular in the collinear limit. An investigation of the numerator factors, using Eqs. (16), (19), (23), and (26), shows that they are indeed nonsingular and therefore do not contribute. Finally, for the term in the three-mass sum where a and b straddle two adjacent massive legs, either A and B, or B and C, there is also no collinear singularity due to the factors of $\langle A_{-1}B_1\rangle$ and $\langle B_{-1}C_1\rangle$ in Eq. (15).

There are also contributions to the loop splitting functions. These terms arise from discontinuities in the integrals, and also from hard two-mass and one-mass box integrals [43]. The latter terms are easily identifiable because the box integral function does not reduce to a daughter integral function (instead it reduces to a contribution to the loop splitting function). The issue of contributions proportional to the loop splitting function is separate from the contributions proportional to the tree splitting function, so it is not directly relevant to determining the lower-point coefficients. (It could of course be used as an additional check on the amplitudes.)

The soft limit, in which the momentum of one gluon is scaled to zero, provides another check on our results. (The soft limit may be phrased in a Lorentz-invariant way as the simultaneous limit $s_{as}, s_{sb} \to 0$ when (a, s, b) are a sequential triplet of external momenta.) This limit also provides an alternative way to obtain the relation (27) between the hard two-mass and three-mass coefficients. The soft limit of an amplitude obeys an equation very similar to that for a collinear limit. At one loop, as $k_s \to 0$,

$$A^{1-\text{loop}}_{n;1}(\ldots, s-1, s, s+1, \ldots) \overset{k_s\to 0}{\to} S^{\text{tree}}(s-1, s^{h_s}, s+1) A^{1-\text{loop}}_{n-1;1}(\ldots, s-1, s+1, \ldots) + S^{1-\text{loop}}(s-1, s^{h_s}, s+1) A^{\text{tree}}_{n-1}(\ldots, s-1, s+1, \ldots), \tag{37}$$

where S^{tree} and $S^{1-\text{loop}}$ are tree and one-loop soft functions. The tree soft functions are just eikonal factors [39],

$$S^{\text{tree}}(a, s^+, b) = \frac{\langle ab\rangle}{\langle as\rangle\langle sb\rangle}, \qquad S^{\text{tree}}(a, s^-, b) = -\frac{[ab]}{[as][sb]}. \tag{38}$$

As was the case for the collinear limits, the contributions proportional to the loop soft functions are easily separated from the ones proportional to the tree soft function. In the $\mathcal{N} = 4$ theory, the loop soft functions arise entirely from discontinuities in the box functions, or from box functions that do not reduce properly (map smoothly) to daughter integral functions. (Discontinuities arise because of infrared divergences [43]). To obtain relations between $(n+1)$- and n-point coefficients using soft limits, we need not consider the loop soft functions. (Again, they can be used to provide additional consistency checks.)

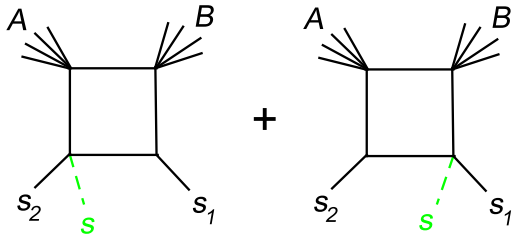

FIG. 6 (color online). The three-mass box integrals that may be used to verify all hard two-mass coefficients. Leg s becomes soft.

Consider now the coefficients of the two three-mass boxes displayed in Fig. 6. As the positive-helicity leg s becomes soft, it is precisely these two box functions that reduce to the hard two-mass box function obtained by simply eliminating leg s. Matching the coefficient of this box function in the soft limit (37) gives the constraint,

$$c^{3m}(s_1, \{s, s_2\}, A, B) + c^{3m}(s_2, A, B, \{s_1, s\}) \overset{k_s\to 0}{\to} S(s_1, s, s_2) c^{2mh}(s_1, s_2, A, B). \tag{39}$$

On the other hand, an inspection of our solution of the three-mass coefficients reveals that

$$c^{3m}(s_1, \{s, s_2\}, A, B) + c^{3m}(s_2, A, B, \{s_1, s\}) \overset{k_s\to 0}{\to} S(s_1, s, s_2) \times (c^{3m}(s_1, \{s_2\}, A, B) + c^{3m}(s_2, A, B, \{s_1\})). \tag{40}$$

Comparing Eqs. (39) and (40) then confirms Eq. (27) for the hard two-mass box in terms of three-mass coefficients.

The behavior of the NMHV amplitudes under multiparticle factorization has an intricate structure which also is useful as a check. Here we do not perform a full analysis, but merely indicate some salient properties. Let K^μ denote the cyclicly-adjacent sum of r momenta given by $K^\mu = (k_i + k_{i+1} + \cdots + k_{i+r-1})^\mu$. The factorization properties for one-loop amplitudes in the limit $K^2 \to 0$ are described by [43],

$$A^{1-\text{loop}}_{n;1} \overset{K^2\to 0}{\longrightarrow} \sum_{h=\pm}\Big[A^{1-\text{loop}}_{r+1;1}(k_i,\ldots,k_{i+r-1},K^h)\frac{i}{K^2}A^{\text{tree}}_{n-r+1}((-K)^{-h},k_{i+r},\ldots,k_{i-1}) + A^{\text{tree}}_{r+1}(k_i,\ldots,k_{i+r-1},K^h)\frac{i}{K^2}A^{1-\text{loop}}_{n-r+1;1}((-K)^{-h},k_{i+r},\ldots,k_{i-1}) + A^{\text{tree}}_{r+1}(k_i,\ldots,k_{i+r-1},K^h)\frac{i}{K^2}A^{\text{tree}}_{n-r+1}((-K)^{-h},k_{i+r},\ldots,k_{i-1})\hat{c}_\Gamma \mathcal{F}_n(K^2;k_1,\ldots,k_n)\Big], \quad (41)$$

where the one-loop *factorization function* $\mathcal{F}_n$ is independent of helicities. (The precise form of $\mathcal{F}_n$ will not concern us here.) For supersymmetric NMHV amplitudes, if the number of negative-helicity gluons in the set $\{i, i+1,\ldots,i+r-1\}$ is either 0 or 3, then the right-hand side of Eq. (41) vanishes. This happens because one of the two amplitudes in each term then has at most one negative-helicity gluon, and such amplitudes are zero in supersymmetric theories. If the number of negative-helicity gluons on one side of the pole is 1 or 2, then exactly one of the two values of the intermediate helicity h gives a nonvanishing contribution to each term in Eq. (41), of the form MHV $\times$ MHV. The box coefficients for the MHV one-loop amplitudes are simply given by the tree amplitude (8) in the case that the box is an easy two-mass, or one-mass box, and zero otherwise [17]. Hence we expect to find a limiting behavior for the NMHV box coefficients of,

$$A^{\text{tree}}_{r+1}(k_i,\ldots,k_{i+r-1},K^h) \times \frac{1}{K^2}A^{\text{tree}}_{n-r+1}((-K)^{-h},k_{i+r},\ldots,k_{i-1}), \quad (42)$$

in appropriate nonvanishing limits.

Before addressing which limits should be nonvanishing, we inspect the two possible sources of multiparticle poles in the building blocks $c^{3\text{m}}$ given in Eq. (15). The first source is the manifest $1/K_B^2$ factor, where B is the mass diagonally opposite the massless leg s. The second source only arises when either mass A or C degenerates to a single massless leg. Suppose A has a single element. Then we can simplify one of the spinorial denominator factors in Eq. (15) to

$$\langle s^-|\not{K}_C\not{K}_B|A^+_{-1}\rangle = \langle s^-|(\not{K}_C+\not{k}_s)(\not{k}_A+\not{K}_B)|A^+\rangle = -(K_C+k_s)^2\langle sA\rangle, \quad (43)$$

exposing the second type of multiparticle pole.

Next we examine the residues of these poles. First suppose all negative helicities are on one side of the pole. In the case of the $1/K_B^2$ pole, this means that either $m_{1,2,3}\in B$, for which $\mathcal{H}$ vanishes according to Eq. (17), or else no negative helicity belongs to B, for which Eqs. (16), (19), and (26) show that the would-be pole is killed by factors of K_B^2 in the numerator $\mathcal{H}^4$. In the case of the $1/(K_C+k_s)^2$ pole from Eq. (43), when all negative helicities are on one side the factor $\mathcal{H}$ vanishes identically, except for the case $m_{1,2}\in B$, $m_3\in A$ in Eq. (20), for which it is proportional to the vanishing denominator: $\langle s^-|\not{K}_C\not{K}_B|m_3^+\rangle = \langle s^-|\not{K}_C\not{K}_B|A^+_{-1}\rangle$. Thus we have verified the "trivial case" where no multiparticle pole was expected.

If one or two negative helicities are on one side of the pole, for either the $1/K_B^2$ pole or the $1/(K_C+k_s)^2$ pole, then we find that such a $c^{3\text{m}}$ coefficient always has the limit (42). For example, if $m_{1,2}\in B$, $m_3\in A$, then in the limit $K_B^2\to 0$ we have,

$$\mathcal{H} = \langle m_1m_2\rangle\langle s^-|\not{K}_C\not{K}_B|m_3^+\rangle \to \langle m_1m_2\rangle\langle s^-|\not{K}_C|B^-\rangle\langle Bm_3\rangle. \quad (44)$$

Because $\langle s^-|\not{K}_A|B^-\rangle = -\langle s^-|\not{K}_C|B^-\rangle$ in this limit, the four spinor strings in the denominator of Eq. (15) cancel the factor of $\langle s^-|\not{K}_C|B^-\rangle^4$ from the numerator. Thus $c^{3\text{m}}$ behaves as,

$$c^{3\text{m}} \to \frac{1}{\langle 12\rangle\langle 23\rangle\cdots\langle n1\rangle K_B^2} \times \frac{\langle m_1m_2\rangle^4\langle Bm_3\rangle^4\langle A_{-1}B_1\rangle\langle B_{-1}C_1\rangle}{\langle BA_{-1}\rangle\langle BB_1\rangle\langle BB_{-1}\rangle\langle BC_1\rangle} = i\frac{\langle Bm_3\rangle^4}{\langle 12\rangle\cdots\langle A_{-1}B\rangle\langle BC_1\rangle\cdots\langle n1\rangle} \times \frac{1}{K_B^2}i\frac{\langle m_1m_2\rangle^4}{\langle(-B)B_1\rangle\cdots\langle B_{-1}(-B)\rangle}, \quad (45)$$

which is the desired form (42). The other partitionings of negative helicities work similarly, for both the $1/K_B^2$ and $1/(K_C+k_s)^2$ poles.

No three-mass boxes appear in the residues of the multiparticle poles, because the $K_B^2\to 0$ limit forces the three-mass boxes containing that pole to become easy two-mass boxes in the daughter amplitude. Indeed, this behavior directly reproduces the daughter easy two-mass boxes where $K=K_B$ is a singlet leg. If instead K is buried in a massive leg of the daughter easy two-mass box, then this type of term typically originates from the $1/K_B^2$ pole in a $c^{3\text{m}}$ contributing to an easy two-mass box coefficient (28) in the parent amplitude. Figure 4, illustrating the double sum for $c^{2\text{m}e}$, exposes the poles: Locations of K counterclockwise from s_1 and clockwise from s_2 generally come from the left sum in Fig. 4 (in the parent amplitude), where K can be identified with K_B for some set B. The ones clockwise from s_1 and counterclockwise from s_2 generally come from the right sum. However, if K is counterclockwise from s_1 and *adjacent* to it (or similarly located with respect to s_2), then K cannot be identified with a K_B. There

is no room for even a single-leg A or C argument. In this case, the daughter term arises from a pole of the type $1/(K_C + k_s)^2$, in a degenerate case of c^{3m} where A or C has a single element. (In the alternative representation of easy two-mass box coefficients with reversed "handedness", the sources of some poles get exchanged.)

Additional checks are possible from other methods of performing the calculation. Very recently, Britto, Cachazo and Feng have found an elegant and effective means for obtaining box coefficients from the quadruple cuts, even when legs of the box integrals are massless, by utilizing a $(--++)$ signature for space-time [36]. We have applied this technique to some of our coefficients, and have found agreement with our direct calculation.

VI. NEW REPRESENTATIONS OF TREE AMPLITUDES

As we have discussed in Sec. III, the infrared consistency equation (14) can be used to compute some of the box coefficients. As we have seen in Sec. IV, it yields a simple and regular form for the resulting coefficients. As a by-product, it also yields a variety of new representations of the n-point tree amplitudes. Because the fermions and scalars do not contribute to n-gluon tree amplitudes, these representations are valid in all massless gauge theories, including QCD. To instantiate one of these representations, we simply collect the coefficients of all boxes with an infrared singularity in any given two-particle invariant. For example, focusing on the $\ln(-s_{12})/\epsilon$ singularity, and inspecting Fig. 7, we obtain, for any helicity configuration, the following form for the n-gluon tree amplitude,

$$2A_n^{\text{tree}} = 2c_{1234} + 2c_{123n} - 2c_{134n} - c_{1345} - c_{13(n-1)n} + \sum_{j=5}^{n-1} c_{123j} - \sum_{j=6}^{n-1} c_{134j} - \sum_{j=5}^{n-2} c_{13jn}. \quad (46)$$

(When an amplitude has more than three negative-helicity gluons, four-mass boxes will appear in the one-loop amplitude, however because these boxes are infrared finite they do not contribute to Eq. (46).) Other representations may be obtained by cyclicly permuting the labels in Eq. (46). We may also shift terms around by using the $n(n-5)/2$ additional identities obtained from the absence of infrared singularities in multiparticle channels, namely $\ln(-s_{i..j})/\epsilon$, $j > i+1$.

These new representations of n-point tree amplitudes have features reminiscent of amplitudes built from CSW diagrams [10]. In particular, for the NMHV case most terms have only a single multiparticle pole, coming from the $1/K_B^2$ in c^{3m} in Eq. (15). The CSW diagrams have the same property. The exception is if a c^{3m} appearing in the expressions for c^{2mh} or c^{2me} in Eqs. (27) and (28) has "degenerate" kinematics where one of the masses vanishes, then, as mentioned in Sec. V, such terms can contain two different multiparticle poles. The appearance of spurious denominators of the form $\langle s^- | \not{K}_C \not{K}_B | A_{-1}^+ \rangle$ is again reminiscent of the CSW approach. (These denominators are "spurious" in the sense that the S-matrix has no singularities corresponding to their vanishing.) However, in the CSW representation of the tree amplitudes, the spurious denominators depend explicitly on a single arbitrary reference momentum η; for example, strings like $\langle C^* B^* \rangle \equiv \langle \eta^+ | \not{K}_C \not{K}_B | \eta^- \rangle$ can appear (although this particular length string first appears in N^2MHV tree amplitudes). In the box-coefficient representation, only physical external momenta appear, and no single external momentum can play the role of η in all terms. The variety of different representations for the tree amplitudes, each with its own set of spurious denominators, suggests the existence of an even more general formalism for obtaining tree amplitudes than the one found by CSW.

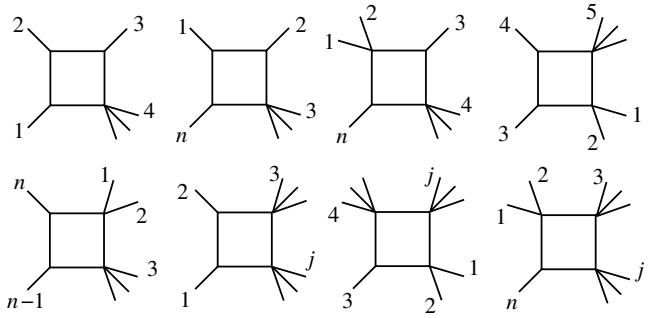

FIG. 7. The boxes whose coefficients combine to give one of the new representations of any one-loop n-point tree amplitude. These boxes are the ones with infrared singularities of the form $\ln(-s_{12})/\epsilon$.

VII. TWISTOR-SPACE PROPERTIES

A. Overview

The target space for Witten's candidate topological string theory is $\mathbb{CP}^{3|4}$, otherwise called projective (super-)twistor space. Points in twistor space correspond to null momenta or equivalently to light cones in space-time. The correspondence is specified by a "half-Fourier" transform. More precisely, if we represent a null momentum by the tensor product of a spinor λ^a and a conjugate spinor $\tilde{\lambda}^{\dot{a}}$, then twistor quantities are obtained by Fourier-transforming with respect to all the $\tilde{\lambda}^{\dot{a}}$.

Amplitudes in twistor space, as it turns out, have rather simple properties. At tree level, they are nonvanishing only on certain curves. This implies that they contain factors of delta functions (or derivatives thereof) whose arguments are the characteristic equations for the curves. The coefficients of the delta functions, however, have been quite difficult to calculate directly from the topological string.

As Witten pointed out in his original paper [1], however, we do not need the twistor-space amplitudes in order to establish the structure of the delta functions they contain.

In momentum space, the Fourier transform turns the characteristic-equation polynomials into differential operators (polynomial in the λ_i, and derivatives with respect to the $\tilde{\lambda}_i$), which will annihilate the amplitude. One particularly useful building block for these differential operators is the line annihilation operator, expressing the condition that three points in twistor space lie on a common "line" or $\mathbb{CP}^1$. If the coordinates of the three points, labeled i, j, k, are $Z_i^I = (\lambda_i^a, \mu_i^{\dot{a}})$, etc., then the appropriate condition is

$$\epsilon_{IJKL} Z_i^I Z_j^J Z_k^K = 0, \tag{47}$$

for all choices of L. Choosing $L = \dot{a}$, and translating this equation back to momentum space using the identification $\mu^{\dot{a}} \leftrightarrow -i\partial/\partial\tilde{\lambda}_{\dot{a}}$, we obtain the operator,

$$F_{ijk} = \langle ij\rangle \frac{\partial}{\partial\tilde{\lambda}_k} + \langle jk\rangle \frac{\partial}{\partial\tilde{\lambda}_i} + \langle ki\rangle \frac{\partial}{\partial\tilde{\lambda}_j}. \tag{48}$$

Two important sufficient conditions for F_{ijk} to annihilate an expression, i.e. for it to have support only when i, j, k lie on a line in twistor space, are [1]

(1) The expression is completely independent of $\tilde{\lambda}_i$, $\tilde{\lambda}_j$, and $\tilde{\lambda}_k$, or
(2) $\tilde{\lambda}_i$, $\tilde{\lambda}_j$, $\tilde{\lambda}_k$ appear only via a sum of momenta containing them, of the form

$$\begin{aligned} P^{a\dot{a}} &= (\cdots + k_i + k_j + k_k + \cdots)^{a\dot{a}} \\ &= \cdots + \lambda_i^a \tilde{\lambda}_i^{\dot{a}} + \lambda_j^a \tilde{\lambda}_j^{\dot{a}} + \lambda_k^a \tilde{\lambda}_k^{\dot{a}} + \cdots \end{aligned} \tag{49}$$

The first condition is obvious from the definition (48); the second holds because of the Schouten identity,

$$\langle ij\rangle\lambda_k + \langle jk\rangle\lambda_i + \langle ki\rangle\lambda_j = 0. \tag{50}$$

The tree-level MHV amplitude (8), for example, is annihilated by F_{ijk}, because it is independent of the $\tilde{\lambda}_i$. Any possible delta functions vanish for generic momenta, because they take the form $\delta(\langle ij\rangle)$. At one loop, Cachazo, Svrček, and Witten [29] pointed out that such delta functions, arising from the spinor analog of the fact that $\partial_{\bar{z}}(1/z) \neq 0$, do arise. They must be taken into account for a proper analysis of the twistor-space structure of amplitudes.

We will not compute the relevant "holomorphic anomaly" terms for the amplitudes in this paper, and so we will not be able to fully exhibit their twistor-space structure. While the "anomaly" terms enter into the action of the differential operators on the box integrals, their action on the coefficients is unaffected by it. The properties of the coefficients are also important, so we focus on these.

In addition to the line operator F_{ijk}, we will employ the planar operator [1],

$$\begin{aligned} K_{ijkl} &\equiv \varepsilon_{IJKL} Z_i^I Z_j^J Z_k^K Z_l^L \\ &= \langle ij\rangle \varepsilon^{\dot{a}\dot{b}} \frac{\partial}{\partial\tilde{\lambda}_k^{\dot{a}}} \frac{\partial}{\partial\tilde{\lambda}_l^{\dot{b}}} \pm [5 \text{ permutations}], \end{aligned} \tag{51}$$

whose vanishing implies that four points lie in a plane (or $\mathbb{CP}^2$) in twistor space.

B. Twistor properties of three-mass box coefficients

As discussed in Sec. IV, the three-mass box coefficients c^{3m} given in Eq. (15) are the basic building blocks for the NMHV amplitudes. All other box coefficients can be expressed as sums of various c^{3m}. Therefore we need only determine the twistor-space properties of the three-mass box coefficients, in order to obtain the general twistor-space properties of all the box coefficients.

The most general twistor-space property of the NMHV box coefficients is that *all points lie in a plane*. That is, K_{mnpq} for every choice of m, n, p, q annihilates every one-term coefficient, and hence, by linearity, it annihilates every box coefficient c_{ijkl}. We first observed the planarity of a special class of three-mass box coefficients in Ref. [23]. The complete coplanarity for all coefficients was proven for general one-loop NMHV amplitudes [23,33], along the same lines used by Cachazo to demonstrate a certain degree of colinearity [31].

Since we have computed all NMHV coefficients, it is straightforward to confirm directly that the required planarity property holds. The coplanarity of s, A, and C can be demonstrated relatively easily, however the coplanarity with B requires more work. In appendix A we present an analytic demonstration of planarity of all three-mass box coefficients. This in turn implies that all remaining coefficients are sums of planar functions since they are sums of three-mass coefficients and their degenerate limits.

Another intriguing property of the nonvanishing coefficients is the universality of the distribution of points on the three lines, independent of the identity of the three negative-helicity legs. As illustrated in Fig. 8, the location of the points is entirely dictated by the three-mass box under consideration. The helicity independence may be understood simply by considering the triple cuts of the

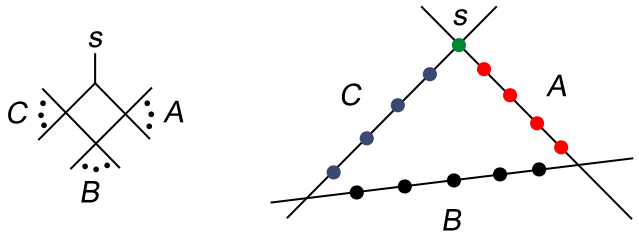

FIG. 8 (color online). The twistor-space configuration for the three-mass-box coefficients c^{3m} given in Eq. (15) is depicted on the right. The corresponding three-mass integral is shown on the left. All points lie in a plane.

three-mass box. As argued by Cachazo [31] for the more standard double cut, the fact that the holomorphic anomaly freezes the phase-space integral [29,30] implies that the box integral coefficients are annihilated by the same collinear operators F_{ijk} that annihilate the trees on either side of the cut. A similar argument for the triple cut shows that the coefficient of a three-mass box must be annihilated by the same collinear operators that annihilate each of the three trees. For all nonvanishing three-mass box coefficients the three tree amplitudes appearing in the triple cut are all MHV. Thus for each of the three clusters A, B and C the points must be on a line, independent of the location of the negative helicities, since this is a property of the MHV tree amplitudes. (The presence of the point s at the intersection of the two lines containing A and C follows from the existence of two distinct triple cuts: one cut where s is a point in the tree amplitude containing the A and one where it is a point in the tree containing the C.) We find it extremely appealing that the simplicity of the structure displayed in Fig. 8 is reflected in the NMHV one-loop amplitudes computed here.

It is worth noting that a similar property holds for the N^{2}MHV (next-to-next-to-MHV) n-point amplitudes. The quadruple cut shows that each cluster in a four-mass box coefficient must always lie on a straight line, since once again each of the four clusters in the quadruple cut is an MHV tree amplitude if the coefficient does not vanish. Moreover, in the triple cut either MHV trees or NMHV trees made up of nearest-neighbor clusters are found. The NMHV trees formed by two nearest-neighbor clusters are supported on two intersecting lines. Stepping through the four triple cuts then implies that nearest-neighbor clusters are localized on intersecting lines. This picture agrees with the properties of the eight-point coefficient of the four-mass box obtained by Britto, Cachazo and Feng [36]. For larger numbers of negative-helicity legs, one can no longer conclude that the points in each cluster lie on straight lines, because the quadruple cuts are no longer products of MHV amplitudes. We may expect the structure of Fig. 9 to generalize, however, with each of the line segments replaced by the twistor-space duals to higher-degree vertices

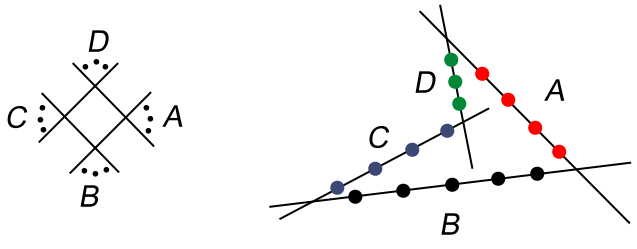

FIG. 9 (color online). The twistor-space configuration for the four-mass-box coefficient of an N^{2}MHV amplitude is depicted on the right. The corresponding four-mass integral is shown on the left. The points need not lie in a plane, but lie in the intersection of two planes.

[14,44], that is appropriate collections of intersecting line segments.

The twistor-space structure of the one- and two-mass box coefficients in the NMHV amplitudes is of course completely determined by the structure of the three-mass coefficients, using eqns. (27), (28), and (33). Each term in these sums will have its support in a plane (that is, a $\mathbb{CP}^2$) in twistor space, though not necessarily the same plane for all terms. Each term has all points lying on three lines within a single plane; and one of the intersections of the lines always contains one of the n points.

VIII. CONCLUSIONS AND OUTLOOK

In this paper we computed all the next-to-MHV one-loop gluon amplitudes in $\mathcal{N} = 4$ super-Yang–Mills theory. The coefficients of the box integral functions appearing in the amplitudes can be written as simple terms built out of spinor strings, or sums of such terms, where each term exhibits a simple twistor-space structure.

To obtain the four-, three- and hard two-mass box coefficients we used generalized cuts [20–23] in the unitarity method [17–20]. The four-mass box coefficients all vanish in the NMHV case, as easily determined from quadruple cuts. We also showed how to obtain hard two-mass box coefficients from the three-mass box coefficients using the known behavior of amplitudes as external momenta become soft. The easy two-mass and one-mass coefficients were then obtained efficiently by solving the constraints that the infrared singularities of the amplitudes (as regulated by dimensional regularization) match the known universal form [26]. We also confirmed some of these coefficients by direct computation of ordinary cuts. For odd n, the infrared consistency equations suffice to obtain all these coefficients. For even n, a lone infrared consistency equation is missing. We computed the missing coefficient from the requirement that amplitudes have the correct collinear limits. The solution to the infrared consistency equations yields a very regular form for the easy two-mass and one-mass coefficients.

We may also apply the structure of the generalized cuts to determine some terms of the corresponding amplitudes in QCD. Many types of integral functions beyond those appearing in the $\mathcal{N} = 4$ results contribute to the full QCD results—scalar triangle integrals, scalar and tensor bubble integrals—and their coefficients are of course undetermined by the calculations in this paper. However, many of the box coefficients are the same as those given in Sec. IV. As a particular example, the coefficient of any box integral where only positive-helicity gluons form one of the massive legs is identical in QCD and the $\mathcal{N} = 4$ theory (and in the pure-glue theory as well).

The infrared consistency equations also provide us with new representations of n-gluon NMHV tree-level amplitudes. The form in which the amplitudes appear is similar to the one obtained using MHV vertices [10]. There are,

however, a number of differences. The variety of different representations for the tree amplitudes, each with their own set of spurious denominators, suggests a more general formalism for obtaining tree amplitudes exists than the one found by Cachazo, Svrček, and Witten.

We also performed a variety of checks, including verifying that amplitudes have the correct behavior in various collinear, soft, and multiparticle factorization limits. As a final check, we also used the observation of Britto, Cachazo, and Feng [36] last week, that generalized quadruple cuts freeze the loop integrals, allowing for an elegant and simple algebraic solution of box coefficients. The utilization of a nonconventional $(--++)$-signature metric, allows quadruple cuts to be applied even when some of the box function's external legs are massless.

The planarity of the NMHV box coefficients is a very intriguing result. The complete planarity was demonstrated for general one-loop NMHV amplitudes [23,33], along the same lines used by Cachazo to demonstrate a certain degree of colinearity [31]. The explicit calculation of the coefficients presented here confirms these arguments. In twistor space, the points in the three-mass box coefficients fall into three lines lying in a plane, and two of the lines always intersect at one of the n points, as depicted in Fig. 8. In particular, the split-up is independent of the particular NMHV helicity configuration, and only depends on the kinematics of the particular three-mass box. As described in the paper, this structure is easy to understand using the generalized cuts together with the twistor-space properties of the tree amplitudes appearing in the cuts.

The simplicity of the amplitudes, found here and in Refs. [17,18,23,31,32,35–37], suggests that the complete one-loop S-matrix of all four-dimensional cut-constructible gauge theories will be obtained soon. Their simple twistor-space structure also suggests the search for a string interpretation will be fruitful.

ACKNOWLEDGMENTS

We thank Radu Roiban, Marcus Spradlin and Anastasia Volovich for helpful discussions on the twistor-space structure of four-mass box coefficients. We also thank Iosif Bena for helpful discussions on general twistor-space properties. We also thank Academic Technology Services at UCLA for computer support. Some of the diagrams in this paper were constructed with JAXODRAW [45]. The *Service de Physique Théorique* is a laboratory of the *Direction des Sciences de la Matière* of the *Commissariat à l'Energie Atomique* of France. This research was supported in part by the US Department of Energy under Contract Nos. DE-FG03-91ER40662 and DE-AC02-76SF00515.

APPENDIX A: EXPLICIT DEMONSTRATION OF PLANARITY OF COEFFICIENTS

The planarity of any box coefficient in any one-loop NMHV amplitude has already been proven on general grounds [23,33]. Nevertheless, it is interesting to see how it works explicitly, now that the complete NMHV results are known. Because every NMHV box coefficient is a sum of the three-mass box coefficients $c^{3\mathrm{m}}$ given in Eq. (15) (and the coplanarity operator K is a linear operator), it suffices to show that this expression is completely planar; that is has its support in a $\mathbb{CP}^2$ subspace.

First we recall the two important sufficient conditions for F_{ijk} to annihilate an expression, described below Eq. (48). Using these, the only way dependence on anti-holomorphic spinors $\tilde{\lambda}_i$ appear in Eq. (15) is via $\not{K}_A$, $\not{K}_B$, and $\not{K}_C$. Furthermore, $\not{K}_A$ and $\not{K}_C$ always appear next to $\langle s^-|$, so that they may be rewritten as $\not{k}_s + \not{K}_A$ and $\not{k}_s + \not{K}_C$, respectively. Thus, using Eq. (49), we see that $c^{3\mathrm{m}}$ in Eq. (15) has support only when all points in each of the following three sets are collinear: $\{s\} \cup A$; B; and $\{s\} \cup C$.

The colinear constraints are shown in Fig. 8. The point s belongs to two lines, A and C. This fact implies that lines A and C lie in a plane. Hence our task is to show that line B also lies in this plane. It suffices to show that

$$K_{a_1 a_2 b_1 b_2} c^{3\mathrm{m}} = 0, \tag{A1}$$

for any two points $a_1, a_2 \in A$ and any two points $b_1, b_2 \in B$. We can use momentum conservation to replace $K_A \to -k_s - K_B - K_C$ in Eq. (15). Then the terms in $K_{a_1 a_2 b_1 b_2}$ containing derivatives with respect to $\tilde{\lambda}_{a_1}$ and $\tilde{\lambda}_{a_2}$ vanish, and Eq. (A1) reduces to

$$\langle a_1 a_2 \rangle \varepsilon^{\dot{\alpha}\dot{\beta}} \frac{\partial}{\partial \tilde{\lambda}^{\dot{\alpha}}_{b_1}} \frac{\partial}{\partial \tilde{\lambda}^{\dot{\beta}}_{b_2}} c^{3\mathrm{m}} = 0. \tag{A2}$$

So we just need to show that the double derivative in Eq. (A2) vanishes.

The first derivative is simple to evaluate, using

$$\frac{\partial}{\partial \tilde{\lambda}^{\dot{\alpha}}_{b_i}} \langle s^-|\not{K}_C \not{K}_B|X^+\rangle = \langle b_i X\rangle (\langle s^-|\not{K}_C)_{\dot{\alpha}}, \tag{A3}$$

$$\frac{\partial}{\partial \tilde{\lambda}^{\dot{\alpha}}_{b_i}} \langle s^-|\not{K}_A \not{K}_B|X^+\rangle = -\langle b_i X\rangle (\langle s^-|\not{K}_C)_{\dot{\alpha}} - \langle sX\rangle (\langle b_i^-|\not{K}_B)_{\dot{\alpha}}, \tag{A4}$$

$$\frac{\partial}{\partial \tilde{\lambda}^{\dot{\alpha}}_{b_i}} K_B^2 = (\langle b_i^-|\not{K}_B)_{\dot{\alpha}}. \tag{A5}$$

The derivative depends on the helicity configuration, through $\mathcal{H}$. Here we will present the most complicated case, $m_1 \in A$, $m_2 \in B$, $m_3 \in C$, for which $\mathcal{H}$ is given by Eq. (21). The other cases can be worked out analogously. We find that

$$\frac{\partial}{\partial \tilde{\lambda}^{\dot{\alpha}}_{b_1}} c^{3\mathrm{m}} = V_{\dot{\alpha}}(b_1) \times c^{3\mathrm{m}}, \tag{A6}$$

where

$$V_{\dot\alpha}(b_1) = \frac{4}{\mathcal{H}}[(\langle m_3 m_2\rangle\langle b_1 m_1\rangle - \langle m_1 m_2\rangle\langle b_1 m_3\rangle)(\langle s^-|\not{K}_C)_{\dot\alpha} - \langle m_1 m_2\rangle\langle s m_3\rangle(\langle b_1^-|\not{K}_B)_{\dot\alpha}] - \frac{(\langle b_1^-|\not{K}_B)_{\dot\alpha}}{K_B^2}$$
$$- \frac{\langle b_1 A_{-1}\rangle(\langle s^-|\not{K}_C)_{\dot\alpha}}{\langle s^-|\not{K}_C\not{K}_B|A_{-1}^+\rangle} - \frac{\langle b_1 B_1\rangle(\langle s^-|\not{K}_C)_{\dot\alpha}}{\langle s^-|\not{K}_C\not{K}_B|B_1^+\rangle} + \frac{\langle b_1 B_{-1}\rangle(\langle s^-|\not{K}_C)_{\dot\alpha} + \langle s B_{-1}\rangle(\langle b_1^-|\not{K}_B)_{\dot\alpha}}{\langle s^-|\not{K}_A\not{K}_B|B_{-1}^+\rangle}$$
$$+ \frac{\langle b_1 C_1\rangle(\langle s^-|\not{K}_C)_{\dot\alpha} + \langle s C_1\rangle(\langle b_1^-|\not{K}_B)_{\dot\alpha}}{\langle s^-|\not{K}_A\not{K}_B|C_1^+\rangle}. \tag{A7}$$

The second derivative has two types of terms,

$$\varepsilon^{\dot\alpha\dot\beta}\frac{\partial}{\partial\tilde\lambda_{b_1}^{\dot\alpha}}\frac{\partial}{\partial\tilde\lambda_{b_2}^{\dot\beta}}c^{3\mathrm{m}} = \Big[\varepsilon^{\dot\alpha\dot\beta}\frac{\partial}{\partial\tilde\lambda_{b_2}^{\dot\beta}}V_{\dot\alpha}(b_1) + \varepsilon^{\dot\alpha\dot\beta}V_{\dot\alpha}(b_1)V_{\dot\beta}(b_2)\Big]\times c^{3\mathrm{m}}, \tag{A8}$$

Note that

$$\varepsilon^{\dot\alpha\dot\beta}(\langle s^-|\not{K}_C)_{\dot\alpha}(\langle s^-|\not{K}_C)_{\dot\beta} = -\langle s^-|\not{K}_C\not{K}_C|s^+\rangle = -K_C^2\langle ss\rangle = 0. \tag{A9}$$

Using this fact, it is easy to see that in the first type of terms—those coming from the derivative of $V_{\dot\alpha}(b_1)$—the terms containing $\langle s^-|\not{K}_C\not{K}_B|X^+\rangle$ do not contribute. The term containing K_B^2 gives

$$\varepsilon^{\dot\alpha\dot\beta}\frac{\partial}{\partial\tilde\lambda_{b_2}^{\dot\beta}}\Big[-\frac{(\langle b_1^-|\not{K}_B)_{\dot\alpha}}{K_B^2}\Big] = \varepsilon^{\dot\alpha\dot\beta}\Big[\frac{1}{(K_B^2)^2}(\langle b_1^-|\not{K}_B)_{\dot\alpha}\times(\langle b_2^-|\not{K}_B)_{\dot\beta} - \frac{1}{K_B^2}(-1)\langle b_1 b_2\rangle\varepsilon_{\dot\beta\dot\alpha}\Big] = \frac{\langle b_1 b_2\rangle}{K_B^2}. \tag{A10}$$

A slightly more complicated term is

$$\varepsilon^{\dot\alpha\dot\beta}\frac{\partial}{\partial\tilde\lambda_{b_2}^{\dot\beta}}\frac{\langle b_1 B_{-1}\rangle(\langle s^-|\not{K}_C)_{\dot\alpha} + \langle s B_{-1}\rangle(\langle b_1^-|\not{K}_B)_{\dot\alpha}}{\langle s^-|\not{K}_A\not{K}_B|B_{-1}^+\rangle} = \varepsilon^{\dot\alpha\dot\beta}\Big\{\frac{1}{\langle s^-|\not{K}_A\not{K}_B|B_{-1}^+\rangle^2}[\langle b_1 B_{-1}\rangle(\langle s^-|\not{K}_C)_{\dot\alpha} + \langle s B_{-1}\rangle(\langle b_1^-|\not{K}_B)_{\dot\alpha}]$$
$$\times[\langle b_2 B_{-1}\rangle(\langle s^-|\not{K}_C)_{\dot\beta} + \langle s B_{-1}\rangle(\langle b_2^-|\not{K}_B)_{\dot\beta}] - \frac{\varepsilon_{\dot\beta\dot\alpha}\langle b_1 b_2\rangle\langle s B_{-1}\rangle}{\langle s^-|\not{K}_A\not{K}_B|B_{-1}^+\rangle}\Big\}$$
$$= -\frac{\langle s B_{-1}\rangle}{\langle s^-|\not{K}_A\not{K}_B|B_{-1}^+\rangle^2}[\langle b_1 B_{-1}\rangle\langle s^-|\not{K}_C\not{K}_B|b_2^+\rangle - \langle b_2 B_{-1}\rangle$$
$$\times\langle s^-|\not{K}_C\not{K}_B|b_1^+\rangle + \langle b_1^-|\not{K}_B\not{K}_B|b_2^+\rangle\langle s B_{-1}\rangle] - 2\frac{\langle b_1 b_2\rangle\langle s B_{-1}\rangle}{\langle s^-|\not{K}_A\not{K}_B|B_{-1}^+\rangle}. \tag{A11}$$

In the quantity in brackets ([]) on the right-hand side of Eq. (A11), we use the Schouten identity to combine the first two terms, and rewrite the third term as $\langle b_1 b_2\rangle\times\langle s^-|\not{K}_B\not{K}_B|B_{-1}^+\rangle$. Then this quantity becomes

$$\langle b_1 b_2\rangle\langle s^-|(\not{K}_C + \not{K}_B)\not{K}_B|B_{-1}^+\rangle = -\langle b_1 b_2\rangle\langle s^-|\not{K}_A\not{K}_B|B_{-1}^+\rangle. \tag{A12}$$

Inserting this expression into Eq. (A11), we obtain,

$$\varepsilon^{\dot\alpha\dot\beta}\frac{\partial}{\partial\tilde\lambda_{b_2}^{\dot\beta}}\frac{\langle b_1 B_{-1}\rangle(\langle s^-|\not{K}_C)_{\dot\alpha} + \langle s B_{-1}\rangle(\langle b_1^-|\not{K}_B)_{\dot\alpha}}{\langle s^-|\not{K}_A\not{K}_B|B_{-1}^+\rangle} = -\frac{\langle b_1 b_2\rangle\langle s B_{-1}\rangle}{\langle s^-|\not{K}_A\not{K}_B|B_{-1}^+\rangle}. \tag{A13}$$

The remaining two nontrivial terms in the derivative of $V_{\dot\alpha}(b_1)$ work very similarly. Assembling all four terms, we have

$$\varepsilon^{\dot\alpha\dot\beta}\frac{\partial}{\partial\tilde\lambda_{b_2}^{\dot\beta}}V_{\dot\alpha}(b_1) = \langle b_1 b_2\rangle\Big[4\frac{\langle m_1 m_2\rangle\langle s m_3\rangle}{\langle s^-|\not{K}_A\not{K}_B|m_3^+\rangle} + \frac{1}{K_B^2} - \frac{\langle s B_{-1}\rangle}{\langle s^-|\not{K}_A\not{K}_B|B_{-1}^+\rangle} - \frac{\langle s C_1\rangle}{\langle s^-|\not{K}_A\not{K}_B|C_1^+\rangle}\Big]. \tag{A14}$$

Terms of the second type arise from the contraction $\varepsilon^{\dot\alpha\dot\beta}V_{\dot\alpha}(b_1)V_{\dot\beta}(b_2)$. There are $5\times5 = 25$ terms, although the terms containing two $\langle s^-|\not{K}_C\not{K}_B|X^+\rangle$ strings do not contribute. In each of the nonvanishing terms, the Schouten identity can again be used to extract a factor of $\langle b_1 b_2\rangle$, and the remainder becomes a sum of two (or sometimes just one) of the terms in Eq. (A14). For example,

using algebra similar to that in Eq. (A11), we get,

$$\varepsilon^{\dot\alpha\dot\beta}\Big[\frac{\langle b_1 B_{-1}\rangle(\langle s^-|\not{K}_C)_{\dot\alpha}+\langle sB_{-1}\rangle(\langle b_1^-|\not{K}_B)_{\dot\alpha}}{\langle s^-|\not{K}_A\not{K}_B|B_{-1}^+\rangle}\,\frac{\langle b_2 C_1\rangle(\langle s^-|\not{K}_C)_{\dot\beta}+\langle sC_1\rangle(\langle b_2^-|\not{K}_B)_{\dot\beta}}{\langle s^-|\not{K}_A\not{K}_B|C_1^+\rangle}+(B_{-1}\leftrightarrow C_1)\Big]$$
$$=\langle b_1 b_2\rangle\Big[\frac{\langle sB_{-1}\rangle}{\langle s^-|\not{K}_A\not{K}_B|B_{-1}^+\rangle}+\frac{\langle sC_1\rangle}{\langle s^-|\not{K}_A\not{K}_B|C_1^+\rangle}\Big]. \tag{A15}$$

Computing and assembling all the $\varepsilon^{\dot\alpha\dot\beta}V_{\dot\alpha}(b_1)V_{\dot\beta}(b_2)$ contributions, we get,

$$\varepsilon^{\dot\alpha\dot\beta}V_{\dot\alpha}(b_1)V_{\dot\beta}(b_2)=\langle b_1 b_2\rangle\Big\{\frac{\langle m_1 m_2\rangle\langle sm_3\rangle}{\langle s^-|\not{K}_A\not{K}_B|m_3^+\rangle}\times[16-4-4-4-4-4]+\frac{1}{K_B^2}\times[4-1-1-1-1-1]$$
$$+\frac{\langle sB_{-1}\rangle}{\langle s^-|\not{K}_A\not{K}_B|B_{-1}^+\rangle}\times[-4+1+1+1+1+1]+\frac{\langle sC_1\rangle}{\langle s^-|\not{K}_A\not{K}_B|C_1^+\rangle}\times[-4+1+1+1+1+1]\Big\}, \tag{A16}$$

where the 6 numbers in each set of brackets correspond to the contribution from the cross term of the term shown with each of the 6 terms in $V_{\dot\alpha}$ in Eq. (A7). The sum of Eqs. (A14) and (A16) is zero, which demonstrates, via Eq. (A8), the planarity of $c^{3\mathrm{m}}$.

APPENDIX B: BOX INTEGRALS

In this appendix we collect the dimensionally-regulated integral functions appearing in the $\mathcal{N}=4$ amplitudes; the first of these integral functions was obtained from Ref. [46] and the remaining ones from Ref. [24]. The reader is referred to these papers for further details. Through $\mathcal{O}(\epsilon^0)$, in the Euclidean region the integral functions are

$$F^{4\mathrm{m}}(s,t,K_1^2,K_2^2,K_3^2,K_4^2)=\frac{1}{2}\Big\{-\mathrm{Li}_2\Big(\frac{1}{2}(1-\lambda_1+\lambda_2+\rho)\Big)+\mathrm{Li}_2\Big(\frac{1}{2}(1-\lambda_1+\lambda_2-\rho)\Big)-\mathrm{Li}_2\Big(-\frac{1}{2\lambda_1}(1-\lambda_1-\lambda_2-\rho)\Big)$$
$$+\mathrm{Li}_2\Big(-\frac{1}{2\lambda_1}(1-\lambda_1-\lambda_2+\rho)\Big)-\frac{1}{2}\ln\Big(\frac{\lambda_1}{\lambda_2^2}\Big)\ln\Big(\frac{1+\lambda_1-\lambda_2+\rho}{1+\lambda_1-\lambda_2-\rho}\Big)\Big\}, \tag{B1}$$

$$F^{3\mathrm{m}}(s,t,K_2^2,K_3^2,K_4^2)=-\frac{1}{2\epsilon^2}[(-s)^{-\epsilon}+(-t)^{-\epsilon}-(-K_2^2)^{-\epsilon}-(-K_4^2)^{-\epsilon}]-\frac{1}{2}\ln\Big(\frac{-K_2^2}{-t}\Big)\ln\Big(\frac{-K_3^2}{-t}\Big)-\frac{1}{2}\ln\Big(\frac{-K_3^2}{-s}\Big)$$
$$\times\ln\Big(\frac{-K_4^2}{-s}\Big)+\mathrm{Li}_2\Big(1-\frac{K_2^2}{s}\Big)+\mathrm{Li}_2\Big(1-\frac{K_4^2}{t}\Big)-\mathrm{Li}_2\Big(1-\frac{K_2^2K_4^2}{st}\Big)+\frac{1}{2}\ln^2\Big(\frac{-s}{-t}\Big), \tag{B2}$$

$$F^{2mh}(s,t,K_3^2,K_4^2)=-\frac{1}{2\epsilon^2}[(-s)^{-\epsilon}+2(-t)^{-\epsilon}-(-K_3^2)^{-\epsilon}-(-K_4^2)^{-\epsilon}]-\frac{1}{2}\ln\Big(\frac{-K_3^2}{-s}\Big)\ln\Big(\frac{-K_4^2}{-s}\Big)+\mathrm{Li}_2\Big(1-\frac{K_3^2}{t}\Big)$$
$$+\mathrm{Li}_2\Big(1-\frac{K_4^2}{t}\Big)+\frac{1}{2}\ln^2\Big(\frac{-s}{-t}\Big), \tag{B3}$$

$$F^{2me}(s,t,K_2^2,K_4^2)=-\frac{1}{\epsilon^2}[(-s)^{-\epsilon}+(-t)^{-\epsilon}-(-K_2^2)^{-\epsilon}-(-K_4^2)^{-\epsilon}]+\mathrm{Li}_2\Big(1-\frac{K_2^2}{s}\Big)+\mathrm{Li}_2\Big(1-\frac{K_2^2}{t}\Big)$$
$$+\mathrm{Li}_2\Big(1-\frac{K_4^2}{s}\Big)+\mathrm{Li}_2\Big(1-\frac{K_4^2}{t}\Big)-\mathrm{Li}_2\Big(1-\frac{K_2^2K_4^2}{st}\Big)+\frac{1}{2}\ln^2\Big(\frac{-s}{-t}\Big), \tag{B4}$$

$$F^{1\mathrm{m}}(s,t,K_4^2)=-\frac{1}{\epsilon^2}[(-s)^{-\epsilon}+(-t)^{-\epsilon}-(-K_4^2)^{-\epsilon}]+\mathrm{Li}_2\Big(1-\frac{K_4^2}{s}\Big)+\mathrm{Li}_2\Big(1-\frac{K_4^2}{t}\Big)+\frac{1}{2}\ln^2\Big(\frac{-s}{-t}\Big)+\frac{\pi^2}{6}, \tag{B5}$$

$$F^{0\mathrm{m}}(s,t)=-\frac{1}{\epsilon^2}[(-s)^{-\epsilon}+(-t)^{-\epsilon}]+\frac{1}{2}\ln^2\Big(\frac{-s}{-t}\Big)+\frac{\pi^2}{2}, \tag{B6}$$

where the k_i denote massless momenta and the K_i massive momenta. The external momentum arguments $K_1, \ldots, K_4$ are sums of external momenta k_i from the n-point amplitude. The kinematic variables appearing in the integrals are

$$s = (k_1 + k_2)^2, \qquad t = (k_2 + k_3)^2, \tag{B7}$$

or with k relabeled as K for off-shell (massive) legs. The functions appearing in $F_4^{4\mathrm{m}}$ are

$$\rho \equiv \sqrt{1 - 2\lambda_1 - 2\lambda_2 + \lambda_1^2 - 2\lambda_1\lambda_2 + \lambda_2^2}, \tag{B8}$$

and

$$\lambda_1 = \frac{K_1^2 K_3^2}{(K_1 + K_2)^2 (K_2 + K_3)^2}, \qquad \lambda_2 = \frac{K_2^2 K_4^2}{(K_1 + K_2)^2 (K_2 + K_3)^2}. \tag{B9}$$

We have rearranged the expressions for $F^{3\mathrm{m}}$ and $F^{2\mathrm{m}h}$ to make the poles in ϵ more transparent. We have also corrected some signs in $F^{4\mathrm{m}}$ in Ref. [17] and in the published version of Ref. [24].

[1] E. Witten, Commun. Math. Phys. **252**, 189 (2004).
[2] R. Roiban, M. Spradlin, and A. Volovich, J. High Energy Phys. 04 (2004) 012; R. Roiban and A. Volovich, Phys. Rev. Lett. **93**, 131602 (2004); R. Roiban, M. Spradlin, and A. Volovich, Phys. Rev. D **70**, 026009 (2004); E. Witten, hep-th/0403199.
[3] V. P. Nair, Phys. Lett. B **214**, 215 (1988).
[4] N. Berkovits, Phys. Rev. Lett. **93**, 011601 (2004).
[5] N. Berkovits and L. Motl, J. High Energy Phys. 04 (2004) 056.
[6] A. Neitzke and C. Vafa, hep-th/0402128.
[7] W. Siegel, hep-th/0404255.
[8] S. J. Parke and T. R. Taylor, Phys. Rev. Lett. **56**, 2459 (1986).
[9] F. A. Berends and W. T. Giele, Nucl. Phys. **B306**, 759 (1988); D. A. Kosower, Nucl. Phys. **335**, 23 (1990).
[10] F. Cachazo, P. Svrček, and E. Witten, J. High Energy Phys. 09 (2004) 006.
[11] G. Georgiou and V. V. Khoze, J. High Energy Phys. 05 (2004) 070; J. B. Wu and C. J. Zhu, J. High Energy Phys. 09 (2004) 063; G. Georgiou, E. W. N. Glover, and V. V. Khoze, J. High Energy Phys. 07 (2004) 048.
[12] D. A. Kosower, Phys. Rev. D **71**, 045007, (2005).
[13] C. J. Zhu, J. High Energy Phys. 04 (2004) 032; J. B. Wu and C. J. Zhu, J. High Energy Phys. 07 (2004) 032; Y. Abe, V. P. Nair, and M. I. Park, Phys. Rev. D **71**, 025002 (2005).
[14] I. Bena, Z. Bern, and D. A. Kosower, Phys. Rev. D **71**, 045008 (2005).
[15] L. J. Dixon, E. W. N. Glover, and V. V. Khoze, J. High Energy Phys. 12 (2004) 015.
[16] Z. Bern, D. Forde, D. A. Kosower, and P. Mastrolia, hep-ph/0412167.
[17] Z. Bern, L. J. Dixon, D. C. Dunbar, and D. A. Kosower, Nucl. Phys. **B425**, 217 (1994).
[18] Z. Bern, L. J. Dixon, D. C. Dunbar, and D. A. Kosower, Nucl. Phys. **B435**, 59 (1995).
[19] Z. Bern and A. G. Morgan, Nucl. Phys. **B467**, 479 (1996); Z. Bern, L. J. Dixon, and D. A. Kosower, Annu. Rev. Nucl. Part. Sci. **46**, 109 (1996); Nucl. Phys. B Proc. Suppl. **51**, 243 (1996).
[20] Z. Bern, L. J. Dixon, and D. A. Kosower, J. High Energy Phys. 08 (2004) 012.
[21] Z. Bern, L. J. Dixon, and D. A. Kosower, Nucl. Phys. **B513**, 3 (1998).
[22] Z. Bern, L. J. Dixon, and D. A. Kosower, J. High Energy Phys. 01 (2000) 027.
[23] Z. Bern, V. Del Duca, L. J. Dixon, and D. A. Kosower, Phys. Rev. D **71**, 045006 (2005).
[24] Z. Bern, L. J. Dixon, and D. A. Kosower, Nucl. Phys. **B412**, 751 (1994).
[25] Z. Bern, L. J. Dixon, and D. A. Kosower, Phys. Lett. B **302**, 299 (1993); **318**, 649E (1993).
[26] W. T. Giele and E. W. N. Glover, Phys. Rev. D **46**, 1980 (1992); Z. Kunszt, A. Signer, and Z. Trócsányi, Nucl. Phys. **B420**, 550 (1994); S. Catani, Phys. Lett. B **427**, 161 (1998).
[27] A. Brandhuber, B. Spence, and G. Travaglini, Nucl. Phys. **B706**, 150 (2005).
[28] F. Cachazo, P. Svrček, and E. Witten, J. High Energy Phys. 10 (2004) 074.
[29] F. Cachazo, P. Svrček, and E. Witten, J. High Energy Phys. 10 (2004) 077.
[30] I. Bena, Z. Bern, D. A. Kosower, and R. Roiban, hep-th/0410054.
[31] F. Cachazo, hep-th/0410077.
[32] R. Britto, F. Cachazo, and B. Feng, Phys. Rev. D **71**, 025012 (2005).
[33] R. Britto, F. Cachazo, and B. Feng, Phys. Lett. B **611**, 167 (2005).
[34] C. Quigley and M. Rozali, J. High Energy Phys. 01 (2005) 053; J. Bedford, A. Brandhuber, B. Spence, and G. Travaglini, Nucl. Phys. **B706**, 100 (2005).
[35] S. J. Bidder, N. E. J. Bjerrum-Bohr, L. J. Dixon, and D. C. Dunbar, Phys. Lett. B **606**, 189 (2005); S. J. Bidder, N. E. J. Bjerrum-Bohr, D. C. Dunbar, and W. B. Perkins, Phys. Lett. B **608**, 151 (2005).
[36] R. Britto, F. Cachazo, and B. Feng, hep-th/0412103.
[37] J. Bedford, A. Brandhuber, B. Spence, and G. Travaglini, Nucl. Phys. **B712**, 59 (2005).
[38] J. E. Paton and H. M. Chan, Nucl. Phys. **B10**, 516 (1969); P. Cvitanovic, P. G. Lauwers, and P. N. Scharbach, Nucl. Phys. **186**, 165 (1981); F. A. Berends and W. Giele, Nucl. Phys. **B294**, 700 (1987); D. Kosower, B. H. Lee, and V. P. Nair, Phys. Lett. B **201**, 85 (1988); M. L. Mangano, S. J.

Parke, and Z. Xu, Nucl. Phys. **B298**, 653 (1988).
[39] M. L. Mangano and S. J. Parke, Phys. Rep. **200**, 301 (1991); L. J. Dixon, in *QCD & Beyond: Proceedings of TASI '95*, edited by D. E. Soper (World Scientific, Singapore, 1996).
[40] F. A. Berends, R. Kleiss, P. De Causmaecker, R. Gastmans, and T. T. Wu, Phys. Lett. B **103**, 124 (1981); P. De Causmaecker, R. Gastmans, W. Troost, and T. T. Wu, Nucl. Phys. **B206**, 53 (1982); Z. Xu, D.-H. Zhang, and L. Chang, Tsinghua University Report No. TUTP–84/3, 1984 (unpublished); R. Kleiss and W. J. Stirling, Nucl. Phys. **B262**, 235 (1985); J. F. Gunion and Z. Kunszt, Phys. Lett. **161B**, 333 (1985); Z. Xu, D.-H. Zhang, and L. Chang, Nucl. Phys. **B291**, 392 (1987).
[41] Z. Bern and D. A. Kosower, Nucl. Phys. **B362**, 389 (1991).
[42] L. M. Brown and R. P. Feynman, Phys. Rev. **85**, 231 (1952); G. Passarino and M. J. G. Veltman, Nucl. Phys. **B160**, 151 (1979).
[43] Z. Bern and G. Chalmers, Nucl. Phys. **B447**, 465 (1995).
[44] S. Gukov, L. Motl, and A. Neitzke, hep-th/0404085.
[45] D. Binosi and L. Theussl, Comput. Phys. Commun. **161**, 76 (2004).
[46] A. Denner, U. Nierste, and R. Scharf, Nucl. Phys. **B367**, 637 (1991).